

UPPER BOUND ON THE TENSOR-TO-SCALAR RATIO IN GUT-SCALE SUPERSYMMETRIC HYBRID INFLATION

MATTHEW CIVILETTI,¹ CONSTANTINOS PALLIS,² AND QAISAR SHAFI¹

¹ *Bartol Research Institute, Department of Physics and Astronomy, University of Delaware, Newark, DE 19716, USA*
e-mail addresses: mcivil@bartol.udel.edu, shafi@bartol.udel.edu

² *Departament de Física Teòrica and IFIC, Universitat de València-CSIC, E-46100 Burjassot, SPAIN*
e-mail address: cpallis@ific.uv.es

ABSTRACT: We explore the upper bound on the tensor-to-scalar ratio r in supersymmetric (F-term) hybrid inflation models with the gauge symmetry breaking scale set equal to the value $2.86 \cdot 10^{16}$ GeV, as dictated by the unification of the MSSM gauge couplings. We employ a unique renormalizable superpotential and a quasi-canonical Kähler potential, and the scalar spectral index n_s is required to lie within the two-sigma interval from the central value found by the Planck satellite. In a sizable region of the parameter space the potential along the inflationary trajectory is a monotonically increasing function of the inflaton, and for this case, $r \lesssim 2.9 \cdot 10^{-4}$, while the spectral index running, $|dn_s/d \ln k|$, can be as large as 0.01. Ignoring higher order terms which ensure the boundedness of the potential for large values of the inflaton, the upper bound on r is significantly larger, of order 0.01, for subplanckian values of the inflaton, and $|dn_s/d \ln k| \simeq 0.006$.

PACs numbers: 98.80.Cq, 12.60.Jv

I. INTRODUCTION

Supersymmetric (SUSY) hybrid inflation based on F-terms, also referred to as *F-term hybrid inflation* (FHI), is one of the simplest and well-motivated inflationary models [1, 2]. It is tied to a renormalizable superpotential uniquely determined by a global $U(1)$ R-symmetry, does not require fine tuned parameters and it can be naturally followed by the breaking of a *Grand Unified Theory* (GUT) gauge symmetry, such as $G_{B-L} = G_{SM} \times U(1)_{B-L}$ [3], where $G_{SM} = SU(3)_C \times SU(2)_L \times U(1)_Y$ is the gauge group of the *Standard Model* (SM), $G_{LR} = SU(3)_C \times SU(2)_L \times SU(2)_R \times U(1)_{B-L}$ [4, 5], and flipped $SU(5)$ [6–9], with gauge symmetry $G_{5X} = SU(5) \times U(1)_X$. Let us clarify, in passing, that the term “GUT” is used in the sense of the gauge coupling unification within *Minimal SUSY SM* (MSSM), although the aforementioned gauge groups are not simple. Such models can arise from string compactifications, see for e.g. Ref. [7, 10]. The embedding of the simplest model of FHI within a higher gauge group may suffer from the production of cosmic defects which can be evaded, though, in the cases of smooth [11] or shifted [12] FHI.

In the simplest implementation of FHI [1], we should note that the potential along the inflationary track is completely flat at tree level. The inclusion of *radiative corrections* (RCs) [1] produce a slope which is needed to drive inflaton towards the SUSY vacuum. In this approximation the predicted scalar spectral index $n_s \simeq 0.98$, is in slight conflict with the latest WMAP [15] and PLANCK [16] data based on the standard power-law cosmological model with *Cold Dark Matter and a cosmological constant* (Λ CDM). Furthermore, the gauge symmetry breaking scale M turns out to be close to (but certainly lower than) its SUSY value, $M_{GUT} \simeq 2.86 \cdot 10^{16}$ GeV.

A more complete treatment which incorporates *supergravity* (SUGRA) corrections [26] with canonical (minimal) Kähler potential, as well as an important soft SUSY breaking term [14, 17], has been shown to yield values for n_s that are fully compatible with the data [15, 16], with M in this case

somewhat lower than the one obtained in Ref. [1]. A reduction of M is certainly welcome if FHI is followed by the breaking of an abelian gauge symmetry, since it helps to reconcile M with the bound [13] placed on it by the non-observation of cosmic strings [17–20].

The minimal FHI scenario described above, while perfectly consistent with the current observations, requires some modification if one desires to incorporate values of M that are comparable or equal to M_{GUT} . This is indispensable in cases where G_{GUT} includes non abelian factors besides G_{SM} , which are expected to disturb the successful gauge coupling unification within MSSM. In this letter, we would like to emphasize that the observationally favored values (close to 0.96) for n_s with M equal to the SUSY GUT scale can be readily achieved within FHI by invoking a specific type of non-minimal Kähler potential, first proposed in Ref. [22]. In particular, a convenient choice of the next-to-minimal and the next-to-next-to-minimal term of the adopted Kähler potential generates [22–24] a positive mass (quadratic) term for the inflaton and a sizeable negative quartic term which assist us to establish FHI of hilltop type [25] in most of the allowed parameter space of the model. Our objectives can also be achieved in smaller regions of the allowed parameter space even with monotonic inflationary potential and therefore complications related to the initial conditions of FHI can be safely eluded. Acceptable n_s values within this set-up are accompanied with an enhancement of the running of n_s , α_s , and the scalar-to-tensor ratio, r , which reach, thereby, their maximal possible values within FHI if we take into account that M ’s larger than M_{GUT} are certainly less plausible. Note, in passing, that the reduction of n_s by generating a negative mass (quadratic) term for the inflaton, as done in Ref. [21], is not suitable for our purposes since M remains well below M_{GUT} .

Below, we briefly review in Sec. II the basics of FHI when it is embedded in nonminimal SUGRA and briefly recall in Sec. III the observational and theoretical constraints imposed on our model. In Sec. IV we exhibit our updated results, and our conclusions are summarized in Sec. V.

II. FHI WITH NONMINIMAL KÄHLER POTENTIAL

1. SPONTANEOUS BREAKING OF G_{GUT} . The standard FHI can be realized by adopting the superpotential

$$W = \kappa S (\bar{\Phi}\Phi - M^2) \quad (1)$$

which is the most general renormalizable superpotential consistent with a continuous R-symmetry [1] under which

$$S \rightarrow e^{i\alpha} S, \bar{\Phi}\Phi \rightarrow \bar{\Phi}\Phi, W \rightarrow e^{i\alpha} W. \quad (2)$$

Here S is a G_{GUT} -singlet left-handed superfield, and the parameters κ and M are made positive by field redefinitions. In our approach $\bar{\Phi}, \Phi$ are identified with a pair of left-handed superfields conjugate under G_{GUT} which break G_{GUT} down to G_{SM} . Indeed, along the D-flat direction $|\bar{\Phi}| = |\Phi|$ and the SUSY potential, V_{SUSY} , extracted (see e.g. ref. [23, 27]) from W in Eq. (1), reads

$$V_{\text{SUSY}} = \kappa^2 (|\Phi|^2 - M^2)^2 + 2|S|^2|\Phi|^2. \quad (3)$$

From V_{SUSY} in Eq. (3) we find that the SUSY vacuum lies at

$$\langle S \rangle = 0 \quad \text{and} \quad |\langle \Phi \rangle| = |\langle \bar{\Phi} \rangle| = M, \quad (4)$$

where the vacuum expectation values of Φ and $\bar{\Phi}$ are developed along their SM singlet type components. As a consequence, W_{HI} leads to the spontaneous breaking of G_{GUT} to G_{SM} . We single out the following two cases:

- $G_{\text{GUT}} = G_{\text{LR}}$ where Φ and $\bar{\Phi}$ belong to the $(1, 1, 2, -1)$ and $(1, 1, 2, 1)$ representation of G_{LR} – cf. Ref. [5, 24]. The symmetry breaking in this case is

$$SU(2)_{\text{R}} \times U(1)_{B-L} \rightarrow U(1)_Y.$$

Therefore, 3 of the 4 generators of $SU(2)_{\text{R}} \times U(1)_{B-L}$ are broken, leading to 3 Goldstone bosons which are absorbed by the 3 gauge bosons which become massive. Among them, W_{R}^{\pm} with masses $m_{W_{\text{R}}^{\pm}} = gM$ correspond to the charged $SU(2)_{\text{R}}$ gauge generators, and one, A , to a linear combination of the $SU(2)_{\text{R}}$ and $U(1)_{B-L}$ generator with mass $m_A = \sqrt{5/2}gM$, where g is the SUSY gauge coupling constant at the GUT scale.

- $G_{\text{GUT}} = G_{5_{\text{X}}}$, where Φ and $\bar{\Phi}$ belong to the $(10, 1)$ and $(\bar{10}, -1)$ representation of $G_{5_{\text{X}}}$ – cf. Ref. [7–9]. In this case, 13 of the 25 generators of $G_{5_{\text{X}}}$ are broken, giving rise via the Higgs mechanism to 13 massive gauge bosons. In particular, 12 gauge bosons which correspond to the generators of $SU(5)$ acquire masses $m_{X_i^{\pm}} = m_{Y_i^{\pm}} = gM$, and one gauge boson associated with a linear combination of the $SU(5)$ and $U(1)_X$ generators acquires a mass $m_A = \sqrt{32/34}gM$ – cf. Ref. [8].

In both cases no topological defects are generated during the breaking of G_{GUT} , in contrast to gauge groups such as $SU(4)_{\text{C}} \times SU(2)_{\text{L}} \times SU(2)_{\text{R}}$, $SU(5)$ or $SO(10)$ which lead to the production of magnetic monopoles.

2. THE INFLATIONARY STAGE. The superpotential W_{HI} in Eq. (1) gives rise to FHI since, for large enough values of $|S|$, there exist a flat direction

$$\bar{\Phi} = \Phi = 0 \quad \text{where} \quad V_{\text{SUSY}}(\Phi = 0) = V_{\text{HI0}} = \kappa^2 M^4. \quad (5)$$

Obviously, V_{HI0} provides us with a constant potential energy density which can be used to drive inflation. The realization of FHI in the context of SUGRA requires a specific Kähler potential, which does not deviate much from the canonical one [17, 26]; further it respects the R symmetry of Eq. (2). Namely we take

$$K = |S|^2 + |\Phi|^2 + |\bar{\Phi}|^2 + \frac{1}{4}k_{4S}\frac{|S|^4}{m_{\text{P}}^2} + \frac{1}{6}k_{6S}\frac{|S|^6}{m_{\text{P}}^4} + \frac{1}{8}k_{8S}\frac{|S|^8}{m_{\text{P}}^6} + \frac{1}{10}k_{10S}\frac{|S|^{10}}{m_{\text{P}}^8} + \frac{1}{12}k_{12S}\frac{|S|^{12}}{m_{\text{P}}^{10}} + \dots \quad (6)$$

where $k_{4S}, k_{6S}, k_{8S}, k_{10S}$ and k_{12S} are positive or negative constants of order unity and the ellipsis represents higher order terms involving the waterfall fields ($\bar{\Phi}$ and Φ) and S . We can neglect these terms since they are irrelevant along the inflationary path. Finally, we include the RCs. These originate from a mass splitting in the $\Phi - \bar{\Phi}$ supermultiplets, caused by SUSY breaking along the inflationary valley [1]. We end up with the following inflationary potential – see e.g. Ref. [23, 24]:

$$V_{\text{HI}} \simeq V_{\text{HI0}} \left(1 + c_{\text{HI}} + \sum_{\nu=1}^5 (-1)^{\nu} c_{2\nu K} \left(\frac{\sigma}{\sqrt{2}m_{\text{P}}} \right)^{2\nu} \right), \quad (7)$$

where $\sigma = \sqrt{2}|S|$ is the canonically (up to the order $|S|^2$) normalized inflaton field. The contribution of RCs read

$$c_{\text{HI}} = \frac{\kappa^2 N}{32\pi^2} \left(2 \ln \frac{\kappa^2 x M^2}{Q^2} + f_{\text{rc}}(x) \right), \quad (8a)$$

where N , for our cases, is the dimensionality of the representations to which $\bar{\Phi}$ and Φ belong. We have $N = 2$ [$N = 10$] when $G_{\text{GUT}} = G_{\text{LR}}$ [$G_{\text{GUT}} = G_{5_{\text{X}}}$]. Also Q is a renormalization scale, $x = \sigma^2/2M^2$, and

$$f_{\text{rc}}(x) = (x+1)^2 \ln(1+1/x) + (x-1)^2 \ln(1-1/x). \quad (8b)$$

The remaining coefficients, $c_{2\nu K}$, in Eq. (7) can be expressed as functions of the k 's in Eq. (6) [23, 24]. From them only the first two play a crucial role during the inflationary dynamics; they are

$$c_{2K} = k_{4S} \quad \text{and} \quad c_{4K} = \frac{1}{2} - \frac{7k_{4S}}{4} + k_{4S}^2 - \frac{3k_{6S}}{2} \quad (9)$$

The residual higher order terms in the expansion of Eq. (7) prevent a possible runaway behavior of the resulting V_{HI} – see point 8 of Sec. III. For completeness, we include also them:

$$c_{6K} = -\frac{2}{3} + \frac{3k_{4S}}{2} - \frac{7k_{4S}^2}{4} + k_{4S}^3 + \frac{10k_{6S}}{3} - 3k_{4S}k_{6S} + 2k_{8S}, \quad (10a)$$

$$c_{8K} = \frac{3}{8} - \frac{5k_{10S}}{2} - \frac{13k_{4S}}{24} + \frac{41k_{4S}^2}{32} - \frac{7k_{4S}^3}{4} + k_{4S}^4 - \frac{13k_{6S}}{4} + \frac{143k_{4S}k_{6S}}{24} - \frac{9k_{4S}^2k_{6S}}{2} + \frac{9k_{6S}^2}{4} - \frac{39k_{8S}}{8} + 4k_{4S}k_{8S}, \quad (10b)$$

$$c_{10K} = -\frac{2}{15} + \frac{32k_{10S}}{5} + 3k_{12S} + \frac{k_{4S}}{24} - 5k_{10S}k_{4S} - \frac{13k_{4S}^2}{24} + \frac{41k_{4S}^3}{32} - \frac{7k_{4S}^4}{4} + k_{4S}^5 + \frac{5k_{6S}}{3} - \frac{29k_{4S}k_{6S}}{6} + \frac{103k_{4S}^2k_{6S}}{12} - 6k_{4S}^3k_{6S} - 5k_{6S}^2 + \frac{27k_{4S}k_{6S}^2}{4} + 5k_{8S} - \frac{67k_{4S}k_{8S}}{8} + 6k_{4S}^2k_{8S} - 6k_{6S}k_{8S}. \quad (10c)$$

Let us note, lastly, that the most important contribution [14] to V_{HI} from the soft SUSY breaking terms of the order of $(1 - 10)$ TeV does not play any essential role in our set-up due to large M 's employed here – cf. Ref. [17].

III. CONSTRAINING THE MODEL PARAMETERS

Under the assumptions that (i) the observed curvature perturbation is generated wholly by σ and (ii) FHI is followed in turn by matter and radiation era, our inflationary set-up can be qualified by imposing a number of observational (1-3) and theoretical (4-8) requirements specified below:

1. The number of e-foldings that the scale $k_* = 0.05/\text{Mpc}$ undergoes during FHI is at least enough to resolve the horizon and flatness problems of standard Big Bang cosmology. Employing standard methods [16, 23], we can derive the relevant condition:

$$N_{\text{HI}*} = \int_{\sigma_f}^{\sigma_*} \frac{d\sigma}{m_{\text{P}}^2} \frac{V_{\text{HI}}}{V'_{\text{HI}}} \simeq 19.4 + \frac{2}{3} \ln \frac{V_{\text{HI}0}^{1/4}}{1 \text{ GeV}} + \frac{1}{3} \ln \frac{T_{\text{rh}}}{1 \text{ GeV}}, \quad (11)$$

where the prime denotes derivation w.r.t. σ , σ_* is the value of σ when k_* crosses outside the horizon of FHI, and σ_f is the value of σ at the end of FHI. This coincides with either the critical point $\sigma_c = \sqrt{2}M$ appearing in the particle spectrum of the $\Phi - \bar{\Phi}$ system during FHI – see Eq. (8b) –, or the value for which one of the slow-roll parameters [28]

$$\epsilon \simeq m_{\text{P}}^2 \left(V'_{\text{HI}} / \sqrt{2} V_{\text{HI}} \right)^2 \quad \text{and} \quad \eta \simeq m_{\text{P}}^2 V''_{\text{HI}} / V_{\text{HI}} \quad (12)$$

exceeds unity. Since the resulting κ values are sizably larger than $(M/m_{\text{P}})^2$ – see next section – we do not expect the production of extra e-foldings during the waterfall regime, which in our case turns out to be nearly instantaneous – cf. Ref. [29].

2. The amplitude A_s of the power spectrum of the curvature perturbation, which is generated during FHI and can be calculated at k_* as a function of σ_* , must be consistent with the data [15, 16], i.e.

$$\sqrt{A_s} = \frac{1}{2\sqrt{3}\pi m_{\text{P}}^3} \frac{V_{\text{HI}}^{3/2}(\sigma_*)}{|V_{\text{HI},\sigma}(\sigma_*)|} \simeq 4.686 \cdot 10^{-5}. \quad (13)$$

3. The (scalar) spectral index n_s , its running, $a_s = dn_s/d \ln k$, and the scalar-to-tensor ratio, r , given by

$$n_s = 1 - 6\epsilon_* + 2\eta_*, \quad (14a)$$

$$\alpha_s = 2(4\eta_*^2 - (n_s - 1)^2)/3 - 2\xi_* \quad \text{and} \quad r = 16\epsilon_*, \quad (14b)$$

where $\xi \simeq m_{\text{P}}^4 V'_{\text{HI}} V'''_{\text{HI}} / V_{\text{HI}}^2$ and all the variables with the subscript $*$ are evaluated at $\sigma = \sigma_*$, must be in agreement with the observational data [15, 16] derived in the framework of the ΛCDM model:

$$n_s = 0.9603 \pm 0.014 \Rightarrow 0.945 \lesssim n_s \lesssim 0.975, \quad (15a)$$

$$\alpha_s = -0.0134 \pm 0.018 \quad \text{and} \quad r < 0.11, \quad (15b)$$

at 95% *confidence level* (c.l.). Limiting ourselves to α_s 's consistent with the assumptions of the power-law ΛCDM model, we further impose the following upper bound:

$$|\alpha_s| \ll 0.01, \quad (16)$$

since, within the cosmological models with running α_s , $|\alpha_s|$'s of order 0.01 are encountered [15, 16].

4. The G_{GUT} breaking scale in Eq. (4) has to be determined by the unification of the MSSM gauge coupling constants, i.e.,

$$gM \simeq 2 \cdot 10^{16} \text{ GeV}, \quad (17)$$

with $g \simeq 0.7$ being the value of the unified gauge coupling constant. Here gM is the mass at the SUSY vacuum, Eq. (4), of the non singlet under G_{SM} gauge bosons W_{R}^{\pm} if $G_{\text{GUT}} = G_{\text{LR}}$ or X^{\pm} and Y^{\pm} if $G_{\text{GUT}} = G_{5x}$ – see Sec. II.

5. The expression of V_{HI} in Eq. (7) is expected to converge at least for $\sigma \sim \sigma_*$. This fact can be ensured if, for $\sigma \sim \sigma_*$, each successive term $c_{2\nu K}$ in the expansion of V_{HI} (and K) Eq. (7) (and Eq. (6)) is smaller than the previous one. In practice, this objective can be easily accomplished if the k 's in Eq. (6) – or Eq. (7) – are sufficiently low.

6. It is reasonable to ask V_{HI} to be bounded from below as $\sigma \rightarrow \infty$. Given our ignorance, however, for the pre-inflationary (i.e. for $\sigma > \sigma_*$) cosmological evolution we do not impose this requirement as an absolute constraint.

7. Depending on the values of the coefficients in Eq. (7), V_{HI} is a either monotonic function of σ or develops a local minimum and maximum. The latter case may jeopardize the implementation of FHI if σ gets trapped near the minimum of V_{HI} . It is, therefore, crucial to indicate the regions where V_{HI} is a monotonically increasing function of σ .

8. Hilltop FHI proceeds such that σ rolls from σ_{max} , which is the point where the maximum of V_{HI} lies, down to smaller values. Therefore a mild tuning of the initial conditions is required [21] in order to obtain acceptable n_s values, since for lower n_s values we must set σ_* closer to σ_{max} . We quantify the amount of tuning in the initial conditions via the quantity [21]:

$$\Delta_{\text{m}*} = (\sigma_{\text{max}} - \sigma_*) / \sigma_{\text{max}}. \quad (18)$$

Large $\Delta_{\text{m}*}$ values correspond to a more natural FHI scenario.

IV. RESULTS

Our inflationary model depends on the parameters:

$$\kappa, k_{4S}, k_{6S}, k_{8S}, k_{10S}, k_{12S}, N, T_{\text{rh}}, \text{ and } \sigma_*,$$

with M fixed from Eq. (17). In our computation, we use as input parameters k_{8S} , k_{10S} and k_{12S} . We also fix $T_{\text{rh}} \simeq 10^9$ GeV, which saturates the conservative gravitino constraint and results in $N_{\text{HI}*} \simeq 50$. Variation of T_{rh} over 1–2 orders of magnitude is not expected to significantly alter our findings – see Eq. (11). We restrict κ and σ_* such that Eqs. (11) and (13) are fulfilled. The restrictions on n_s from Eq. (15a) can be met by adjusting k_{4S} and k_{6S} , whereas the last three parameters of K control mainly the boundedness and the monotonicity of V_{HI} ; we thus take them into account only if we impose restriction 6 of Sec. III. In these cases we set $k_{10S} = -1$ and $k_{12S} = 0.5$ throughout and we verify that these values do not play a crucial role in the inflationary dynamics. We briefly comment on the impact of the variation of k_{8S} and N on our results. Using Eq. (14b) we can extract α_s and r .

Following the strategy of Ref. [22] we choose the sign of $c_{2K} = k_{4S}$ to be negative – cf. Ref. [21]. As a consequence, fulfilling of Eq. (15a) requires a negative c_{4K} or positive k_{6S} – see Eq. (9). More explicitly, V_{HI} given by Eq. (7) can be approximated as

$$V_{\text{HI}} \simeq V_{\text{HI}0} \left(1 + c_{\text{HI}} + |c_{2K}| \frac{\sigma^2}{2m_{\text{P}}^2} - |c_{4K}| \frac{\sigma^4}{4m_{\text{P}}^4} - |c_{6K}| \frac{\sigma^6}{8m_{\text{P}}^6} + |c_{8K}| \frac{\sigma^8}{16m_{\text{P}}^8} \right), \quad (19)$$

and it may develop a non-monotonic behavior in a sizable portion of the allowed parameter space. Employing Eq. (19), we can show that V_{HI} reaches a local maximum at the inflaton-field value:

$$\sigma_{\text{max}} \simeq \frac{m_{\text{P}} \sqrt{\pi |c_{2K}| + \sqrt{\pi^2 c_{2K}^2 + N \kappa^2 |c_{4K}|}}}{\sqrt{2\pi |c_{4K}|}}, \quad (20a)$$

and a local minimum at the inflaton-field value:

$$\sigma_{\text{min}} \simeq m_{\text{P}} \frac{\sqrt{3 |c_{6K}| + \sqrt{9 c_{6K}^2 + 32 |c_{4K} c_{6K}|}}}{2 \sqrt{|c_{8K}|}}. \quad (20b)$$

In deriving Eq. (20a) we keep terms up to the fourth power of σ in Eq. (19), whereas for Eq. (20b) we focus on the last three terms of the expansion in the right-hand side of Eq. (19). For this reason, the latter result is independent of c_{HI} and c_{2K} .

The structure of V_{HI} is displayed in Fig. 1 where we show the variation of V_{HI} as a function of σ for $\kappa = 0.018$ and $k_{4S} = -0.0443, k_{6S} = 0.736, k_{8S} = -1.5$ (gray line) or $k_{4S} = -0.0415, k_{6S} = 0.656, k_{8S} = -0.5$ (light gray line). These parameters yield $n_s = 0.96$, $r \simeq 0.00019$ and $\alpha_s \simeq 0.0054$ [$\alpha_s \simeq 0.0037$] (gray [light gray] line). The values of $\sigma_*/M \simeq 19.03$ [$\sigma_*/M \simeq 18.4$] (gray [light gray] line) and $\sigma_f/M \simeq 1.42$ are also depicted. In the first case

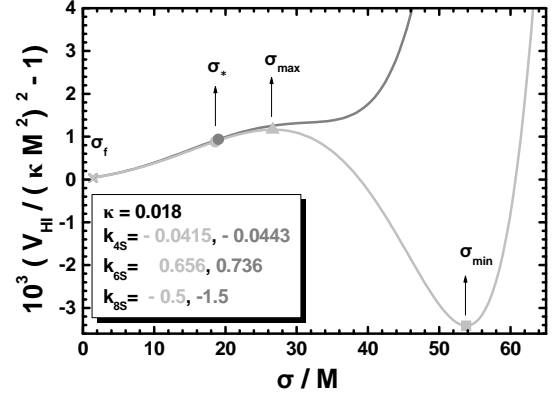


FIG. 1: The variation of V_{HI} in Eq. (19) as a function of σ for $n_s = 0.96$ taking $N = 10$, $\kappa = 0.018$, $k_{10S} = -1$, $k_{12S} = 0.5$ and $k_{4S} = -0.0443, k_{6S} = 0.736, k_{8S} = -1.5$ [$k_{4S} = -0.0415, k_{6S} = 0.656, k_{8S} = -0.5$] (gray [light gray] line). The values of $\sigma_*, \sigma_f, \sigma_{\text{max}}$ and σ_{min} are also depicted.

(gray line) V_{HI} remains monotonic due to the larger $|k_{8S}|$ value employed. Contrarily, V_{HI} develops the minimum-maximum structure, in the second case (light gray line) with the maximum located at $\sigma_{\text{max}}/M = 26.6$ {27.2} and the minimum at $\sigma_{\text{min}}/M = 53.8$ {63.5} – the values obtained via Eqs. (20a) and (20b) are indicated in curly brackets. We find that $\Delta_{\text{m}*} \simeq 0.31$.

Confronting FHI with the constraints of Sec. III, we can identify the allowed regions in the $\kappa - (-k_{4S})$, $\kappa - k_{6S}$, $\kappa - |\alpha_s|$ and $\kappa - r$ planes – see Fig. 2. The conventions adopted for the various lines are also shown. In particular, the thick and thin gray dashed [dot-dashed] lines correspond to $n_s = 0.975$ [$n_s = 0.946$], whereas the thick and thin gray solid lines are obtained by fixing $n_s = 0.96$ – see Eq. (15a). The thick lines are obtained setting $k_{8S} = -1.5$ which – together with the universally selected k_{10S} and k_{12S} above – ensures the fulfilment of restriction 6 of Sec. III; the faint lines correspond to the choice $c_{6K} = c_{8K} = c_{10K} = 0$, which does not ensure the boundedness of V_{HI} . From the panels (a), (b) and (c) we see that the thin lines almost coincide with the thick ones for $\kappa \leq 0.01$, and then deviate and smoothly approach some plateau. The regions allowed by imposing the constraints 1-6 of Sec. III are denoted by light gray shading. In the hatched subregions, requirement 7 is also met. On the other hand, the regions surrounded by the thin lines are actually the allowed ones, when only the restrictions 1-5 of Sec. III are satisfied. The various allowed regions are cut at low κ values since the required k_{6S} reaches rather high values (of order 10), which starts looking unnatural. At the other end, Eq. (16) and $\sigma_* \simeq m_{\text{P}}$ bounds the allowed areas in the case of bounded or unbounded V_{HI} respectively. For both cases, we remark that $|k_{4S}|$ increases with κ whereas k_{6S} drops as κ increases. For fixed κ , increasing $|k_{4S}|$ means decreasing k_{6S} . Moreover, $|k_{4S}|$ is restricted to somewhat small values in order to avoid the well-known [27, 28] η problem of FHI. On the other hand, no tuning for k_{6S} is needed since it is of order unity for most κ values.

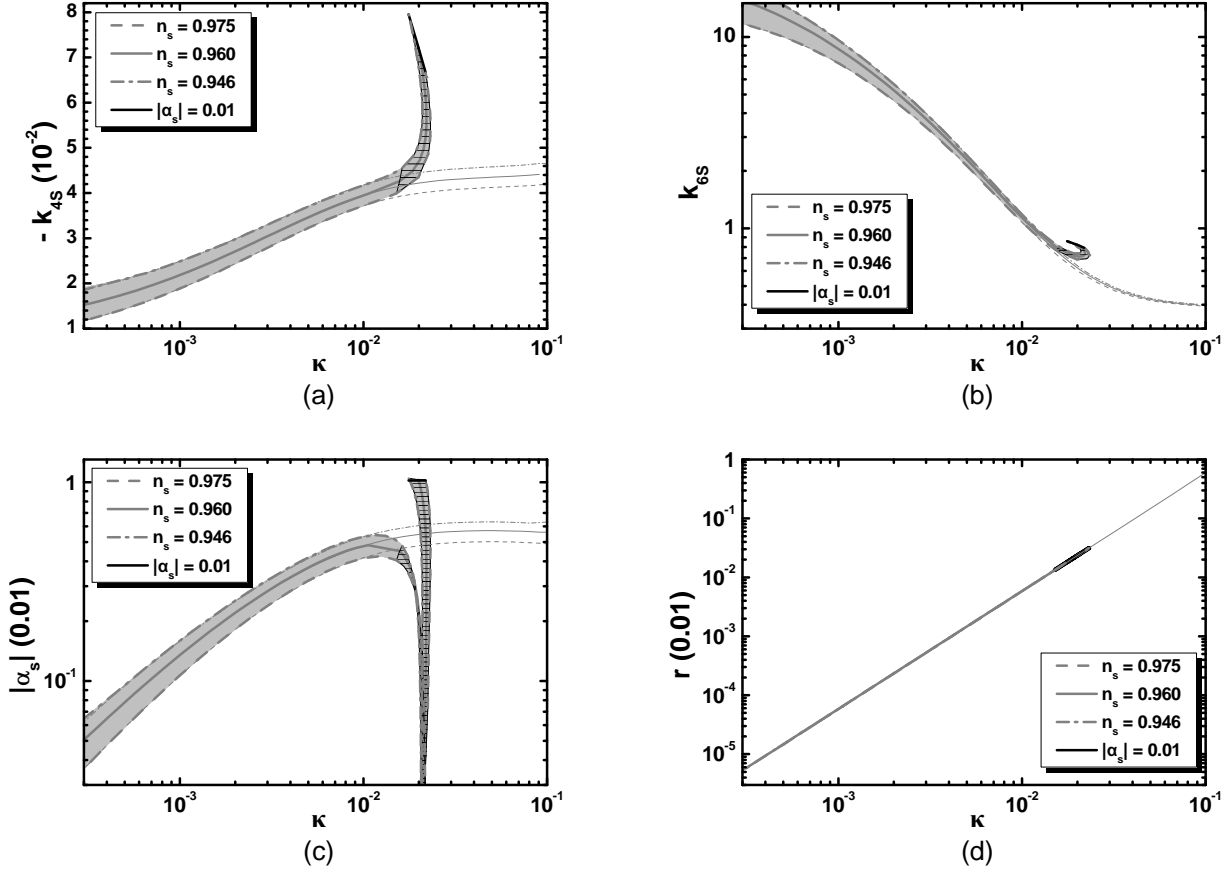


FIG. 2: Allowed (lightly gray shaded) region, as determined by the restrictions 1-6 of Sec. III, in the $\kappa - (-k_{4S})$ (a), $\kappa - k_{6S}$ (b), $\kappa - |\alpha_s|$ (c) and $\kappa - r$ (d) plane for $N = 10$, $k_{8S} = -1.5$, $k_{10S} = -1$ and $k_{12S} = 0.5$. In the hatched regions V_{HI} remains monotonic. The conventions adopted for the various lines are also shown. The thin lines are obtained by setting $c_{6K} = c_{8K} = c_{10K} = 0$ in Eq. (7).

From Fig. 2-(c) we observe that for increasing κ beyond 0.01, $|\alpha_s|$ corresponding to the bold lines precipitously drops at $\kappa \simeq 0.02$, changes sign and rapidly saturates the bound of Eq. (16) along the thick black solid line. In other words, for every κ in the vicinity of $\kappa \simeq 0.2$ we have two acceptable k_{6S} values, as shown in Fig. 2-(b) with two different α_s values of either sign. Furthermore, from Fig. 2-(d) we remark that r is largely independent of the n_s value, and so the various types of lines coincide for both bound and unbounded V_{HI} . We also see that r increases almost linearly with κ and reaches its maximal value which turns out to be: (i) $r \simeq 2.9 \cdot 10^{-5}$ as α_s approaches the bound of Eq. (16), for bounded V ; (ii) $r \simeq 0.01$ as the inequality $\sigma_* \leq m_P$ is saturated for $n_s \simeq 0.975$ and unbounded V_{HI} . Therefore, lifting restriction 6 of Sec. III allows larger r . However, non vanishing $c_{\nu K}$'s perhaps corresponds to a more natural scenario.

We observe that the optimistic restriction 7 in Sec. III can be met in very limited slices of the allowed (lightly gray shaded) areas, only when the boundedness of V_{HI} has been ensured. In these regions σ_* also turns out to be rather large ($10M$), and we therefore observe a mild dependence of our results on c_{6K} (or k_{8S}). This point is further clarified in Table I where we list the model parameters and predictions for $n_s \simeq 0.96$,

$N = 10$, $\kappa = 0.005, 0.01, 0.02$ and various k_{8S} values. We remark that for $\kappa = 0.005$ the results are practically unchanged for varying k_{8S} . The dependence on k_{8S} starts to become relevant for $\kappa \simeq 0.01$ and crucially affects the results for $\kappa = 0.02$; here, for $k_{8S} = -2$ the solution obtained belongs to

TABLE I: Model parameters and predictions for $N = 10$ and $n_s \simeq 0.96$. We take $k_{10S} = -1$, $k_{12S} = 0.5$ and various k_{8S} 's.

$-k_{8S}$	κ (10^{-2})	σ_*/M	k_{4S} (10^{-2})	k_{6S}	Δ_{m*} (%)	α_s (10^{-3})	r (10^{-5})
0.5	0.5	6.7	3.46	2.29	28	3.7	1.5
0.5	1	11.7	3.94	1.04	29	5	6.6
0.5	2	20.4	4.2	0.61	—	5.3	23
1.5	0.5	6.7	3.46	2.29	28	3.7	1.5
1.5	1	11.5	3.98	1.1	30	4.8	5.9
1.5	2	23.64	4.68	0.715	—	2.16	23.6
2.	0.5	6.7	3.46	2.29	28	3.7	1.5
2.	1	11.54	3.98	1.11	30	4.7	6.3
2.	2	23.4	5.2	0.785	—	-8.3	23

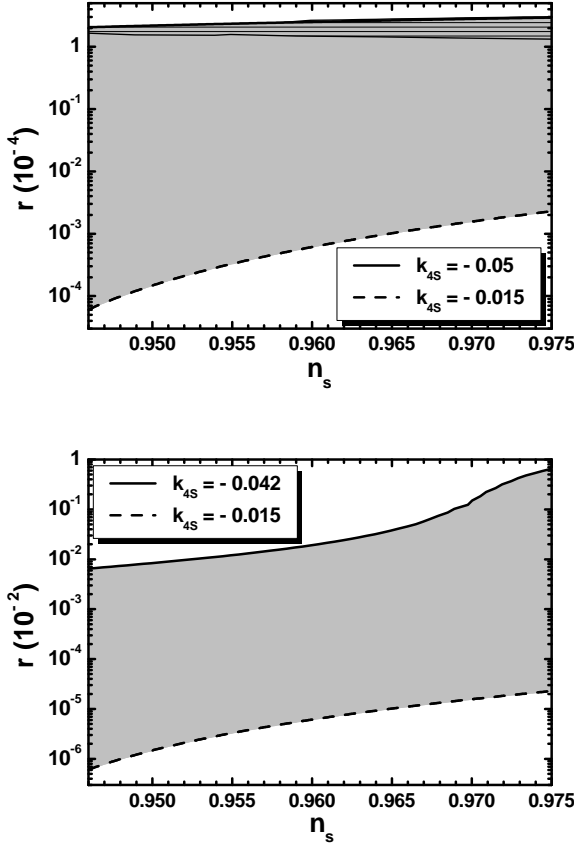


FIG. 3: Variation of r as a function of n_s for $N = 10$. We set $k_{8S} = -1.5$, $k_{10S} = -1$, $k_{12S} = 0.5$, $k_{4S} = -0.05$ (solid line) and $k_{4S} = -0.015$ (dashed line) for the upper plot. For the lower plot we set $c_{6K} = c_{8K} = c_{10K} = 0$ and $k_{4S} = -0.042$ (solid line) or $k_{4S} = -0.015$ (dashed line). The shaded region between the two curves is approximately the allowed region. Hatched is the region in which V_{HI} remains monotonic.

the branch with $\alpha_s < 0$ and not in the branch with $\alpha_s > 0$, as is the case with $\kappa = 0.005$ and 0.01 . Listed is also the quantity Δ_{m*} which takes rather natural values for the selected κ – the entries without a value assigned indicate that V_{HI} is a monotonic function of σ .

As shown in Fig. 2-(a), $|k_{4S}|$ ranges between about 0.015 and 0.05 for the case with bounded V_{HI} or 0.042 for unbounded V_{HI} . For each of these k_{4S} values and every κ in the allowed range found in Fig. 2, we vary k_{6S} in order to obtain n_s in the observationally favored region of Eq. (15a) and we extract the resulting r . Our results are presented in Fig. 3, where we display the allowed region in the $n_s - r$ plane for bounded (upper plot) or unbounded (lower plot) V_{HI} . Along the dashed lines of both plots k_{6S} ranges between 9 and 26 whereas along the solid line of the upper [lower] plot k_{6S} varies between 0.69 and 0.75 [0.39 and 1.15]. From the upper plot we see that the maximal for r is about $2.9 \cdot 10^{-4}$ and turns out to be nearly independent of n_s . Interestingly, this value is included in the region with monotonic V_{HI} depicted by the hatched region. From the lower plot we see that there

TABLE II: Model parameters and predictions for $N = 2$ and $n_s \simeq 0.96$. We set $k_{8S} = -1.5$, $k_{10S} = -1$ and $k_{12S} = 0.5$.

κ (10^{-2})	σ_*/M	$-k_{4S}$ (10^{-2})	k_{6S}	Δ_{m*} (%)	α_s (10^{-4})	r (10^{-5})
0.5	6.4	3.65	2.545	28	4.1	1.5
1	10.4	4.35	1.315	30	5.7	6.2
2	17.3	5.1	0.816	35	6.3	23

is a mild dependence of the largest r from n_s ; thus, the maximal $r = 0.006$ is achieved for $n_s = 0.975$. No region with monotonic V_{HI} is located in this case, however.

Summarizing our findings from Figs. 2 and 3 for n_s in the range given by Eq. (15a) and imposing the restrictions 1-7 of Sec. III, the various quantities are bounded as follows:

$$\{4.9 \cdot 10^{-2}\} 1.5 \lesssim \frac{\kappa}{10^{-2}} \lesssim 2.3, \quad (21a)$$

$$\{1.4\} 4 \lesssim \frac{-k_{4S}}{10^{-2}} \lesssim 7.95, \quad (21b)$$

$$0.68 \lesssim k_{6S} \lesssim 0.77 \{10\}, \quad (21c)$$

$$\{5.7 \cdot 10^{-2}\} 0.4 \lesssim \frac{|\alpha_s|}{10^{-2}} \lesssim 1, \quad (21d)$$

$$\{1.7 \cdot 10^{-3}\} 1.3 \lesssim \frac{r}{10^{-4}} \lesssim 2.9. \quad (21e)$$

Note that the limiting values obtained without imposing the monotonicity of V_{HI} – requirement 7 in Sec. III – are indicated in curly brackets. In the corresponding region, Δ_{m*} ranges between 16 and 32%. As can be deduced from the data of Fig. 2, Δ_{m*} increases with κ 's. Small Δ_{m*} values indicate a second mild tuning (besides the one needed to avoid the η problem), which is however a common feature in the models of hilltop inflation. If we ignore requirement 6 of Sec. III, then confining n_s in the range of Eq. (15a) we obtain the following ranges:

$$4.9 \cdot 10^{-3} \lesssim \frac{\kappa}{10^{-1}} \lesssim 1, \quad (22a)$$

$$1.4 \lesssim \frac{-k_{4S}}{10^{-2}} \lesssim 4.7, \quad (22b)$$

$$0.4 \lesssim k_{6S} \lesssim 10, \quad (22c)$$

$$5.7 \cdot 10^{-1} \lesssim \frac{|\alpha_s|}{10^{-3}} \lesssim 6, \quad (22d)$$

$$1.4 \cdot 10^{-5} \lesssim \frac{r}{10^{-2}} \lesssim 1. \quad (22e)$$

Obviously, no solutions with monotonic V_{HI} are achieved in this case whereas Δ_{m*} varies between 16 and 29%. The maximal r is reached for the maximal n_s in Eq. (15a) and as $\sigma_* \sim m_P$.

So far we focused on G_{5X} , employing $N = 10$ in our investigation. However, our results are not drastically affected even in the case of G_{LR} for most values of κ , as can be inferred by comparing the results (for $k_{8S} = -1.5$) listed in Tables I and II where we use $N = 10$ and $N = 2$ respectively. This signals the fact that the SUGRA corrections to V_{HI} originating from the last term in the sum of Eq. (7) dominate over the radiative

corrections which are represented by c_{HI} . The discrepancy between the two results ranges from 6 to 20%, increasing with κ , and it is essentially invisible in the plots of Fig. 2. On the other hand, we observe that in the $N = 10$ case the enhanced c_{HI} creates a relatively wider space with monotonic V_{HI} ; this space is certainly smaller for $N = 2$, as shown from our outputs for $\kappa = 0.02$.

V. CONCLUSIONS

Inspired by the recently released results by the PLANCK collaboration on the inflationary observables, we have reviewed and updated the nonminimal version of SUSY hybrid inflation arising from F-terms, also referred to as FHI. In our formulation, FHI is based on a unique renormalizable superpotential, employs an quasi-canonical Kähler potential and is followed by the spontaneous breaking at M_{GUT} of a GUT symmetry which is taken to be G_{LR} or $G'_{5\text{x}}$. As suggested first in Ref. [22] and further exemplified in Ref. [23, 24], n_s values close to 0.96 in conjunction with the fulfilment of Eq. (17) can be accommodated by considering an expansion of the Kähler potential – see Eq. (6) – up to twelfth order in powers of the various fields with suitable choice of signs for the coefficients k_{4S} and k_{6S} .

Fixing n_s at its central value, we obtain $\{7.8 \cdot 10^{-2}\} 1.57 \lesssim \kappa/10^{-2} \lesssim 2.2$ with $\{2\} 4.2 \lesssim -k_{4S}/10^{-2} \lesssim 7.2$ and $0.72 \lesssim k_{6S} \lesssim 0.79 \{10\}$, while $|\alpha_s|$ and r assume the values $(\{0.1\} 0.45 - 1) \cdot 10^{-2}$ and $(\{3.5 \cdot 10^{-3}\} 1.4 - 1.9) \cdot 10^{-4}$ respectively – recall that the limiting values in the curly brackets are achieved without imposing the monotonicity of V_{HI} . With a non-monotonic V_{HI} , $\Delta_{\text{m}*}$ ranges between 16 and 30%. It is gratifying that there is a sizable portion of the allowed parameter space where V_{HI} remains a monotonically increasing function of σ ; thus, unnatural restrictions on the initial conditions for inflation due to the appearance of a maximum and a minimum of V_{HI} can be avoided. On the other hand, if we do not insist on the boundedness of V_{HI} , κ reaches 0.1 with $k_{4S} = -0.046$ and $k_{6S} = 0.4$ with the resulting α_s and r being both 0.006, that is close to 0.01. Finally FHI can be followed by a successful scenario of non-thermal leptogenesis [30] for both G_{GUT} 's considered here – cf. Ref. [9, 24].

ACKNOWLEDGMENTS

M.C. and Q.S. acknowledge support by the DOE grant No. DE-FG02-12ER41808. CP acknowledges support from the Generalitat Valenciana under grant PROMETEOII/2013/017.

REFERENCES

- [1] G.R. Dvali, Q. Shafi and R.K. Schaefer, *Phys. Rev. Lett.* **73**, 1886 (1994) [hep-ph/9406319].
- [2] E.J. Copeland *et al.*, *Phys. Rev. D* **49**, 6410 (1994) [astro-ph/9401011].
- [3] V.N. Şenoğuz and Q. Shafi, hep-ph/0512170.
- [4] G.R. Dvali, G. Lazarides and Q. Shafi, *Phys. Lett. B* **424**, 259 (1998) [hep-ph/9710314].
- [5] G. Lazarides and N.D. Vlachos, *Phys. Lett. B* **441**, 46 (1998) [hep-ph/9807253]; G. Lazarides and N.D. Vlachos, *Phys. Lett. B* **459**, 482 (1999) [hep-ph/9903511].
- [6] S.M. Barr, *Phys. Lett. B* **112**, 219 (1982).
- [7] I. Antoniadis, J.R. Ellis, J.S. Hagelin and D.V. Nanopoulos, *Phys. Lett. B* **194**, 231 (1987).
- [8] A.-C. Davis and N.F. Lepora, *Phys. Rev. D* **52**, 7265 (1995) [hep-ph/9504411].
- [9] B. Kyae and Q. Shafi, *Phys. Lett. B* **635**, 247 (2006) [hep-ph/0510105].
- [10] I. Antoniadis, G.K. Leontaris, and N.D. Tracas, *Phys. Lett. B* **279**, 58 (1992); G.K. Leontaris and N.D. Tracas, *ibid.* **291**, 44 (1992).
- [11] G. Lazarides and C. Panagiotakopoulos, *Phys. Rev. D* **52**, R559 (1995) [hep-ph/9506325]; G. Lazarides, C. Panagiotakopoulos, and N.D. Vlachos, *ibid.* **54**, 1369 (1996) [hep-ph/9606297]; R. Jeannerot, S. Khalil, and G. Lazarides, *Phys. Lett. B* **506**, 344 (2001) [hep-ph/0103229]; M. ur Rehman and Q. Shafi, *Phys. Rev. D* **86**, 027301 (2012) [arXiv:1202.0011]; S. Khalil, Q. Shafi, and A. Sil, *ibid.* **86**, 073004 (2012) [arXiv:1208.0731].
- [12] R. Jeannerot, S. Khalil, G. Lazarides, and Q. Shafi, *J. High Energy Phys.* **10**, 012 (2000) [hep-ph/0002151]; S. Khalil, M. ur Rehman, Q. Shafi, and E.A. Zaakouk, *Phys. Rev. D* **83**, 063522 (2011) [arXiv:1104.4143]; M. Civeletti, M. ur Rehman, Q. Shafi, and J.R. Wickman, *ibid.* **84**, 103505 (2011) [arXiv:1010.3657].
- [13] P.A.R. Ade *et al.* [Planck Collaboration], arXiv:1303.5085.
- [14] V.N. Şenoğuz and Q. Shafi, *Phys. Rev. D* **71**, 043514 (2005) [hep-ph/0412102]; M.U. Rehman, Q. Shafi and J.R. Wickman, *Phys. Lett. B* **683**, 191 (2010) [arXiv:0908.3896].
- [15] G. Hinshaw *et al.* [WMAP Collaboration], arXiv:1212.5226.
- [16] P.A.R. Ade *et al.* [Planck Collaboration], arXiv:1303.5082.
- [17] C. Pallis and Q. Shafi, *Phys. Lett. B* **725**, 327 (2013) [arXiv:1304.5202].
- [18] J. Rocher and M. Sakellariadou, *J. Cosmol. Astropart. Phys.* **03**, 004 (2005) [hep-ph/0406120]; R. Jeannerot and M. Postma, *J. High Energy Phys.* **05**, 071 (2005) [hep-ph/0503146].
- [19] K. Nakayama *et al.*, *J. Cosmol. Astropart. Phys.* **12**, 010 (2010) [arXiv:1007.5152].
- [20] W. Buchmüller, V. Domcke and K. Schmitz, *Nucl. Phys.* **B862**, 587 (2012) [arXiv:1202.6679].
- [21] M. Bastero-Gil, S.F. King, and Q. Shafi, *Phys. Lett. B* **651**, 345 (2007) [hep-ph/0604198]; B. Garbrecht *et al.*, *J. High Energy Phys.* **12**, 038 (2006) [hep-ph/0605264]; M.U. Rehman, V.N. Şenoğuz, and Q. Shafi, *Phys. Rev. D* **75**, 043522 (2007) [hep-ph/0612023].
- [22] M.U. Rehman, Q. Shafi and J.R. Wickman, *Phys. Rev. D* **83**, 067304 (2011) [arXiv:1012.0309].
- [23] R. Armillis and C. Pallis, “Recent Advances in Cosmology”, edited by A. Travena and B. Soren (Nova Science Publishers Inc., New York, 2013) [arXiv:1211.4011].
- [24] R. Armillis, G. Lazarides and C. Pallis, *Phys. Rev. D (in press)* [arXiv:1309.6986].
- [25] L. Boubekeur and D. Lyth, *J. Cosmol. Astropart. Phys.* **07**,

- 010 (2005); K. Kohri, C.M. Lin, and D.H. Lyth, *ibid.* **12**, 004 (2007); C.M. Lin and K. Cheung, *ibid.* **03**, 012 (2009).
- [26] A.D. Linde and A. Riotto *Phys. Rev. D* **56**, 1841 (1997) [hep-ph/9703209]; V.N. Şenoğuz and Q. Shafi, *Phys. Lett. B* **567**, 79 (2003) [hep-ph/0305089].
- [27] G. Lazarides, *Lect. Notes Phys.* **592**, 351 (2002) [hep-ph/0111328]; G. Lazarides, *J. Phys. Conf. Ser.* **53**, 528 (2006) [hep-ph/0607032].
- [28] D.H. Lyth and A. Riotto, *Phys. Rept.* **314**, 1 (1999) [hep-ph/9807278]; A. Mazumdar and J. Rocher, *Phys. Rept.* **497**, 85 (2011) [arXiv:1001.0993].
- [29] S. Clesse, *Phys. Rev. D* **83**, 063518 (2011) [arXiv:1006.4522]; H. Kodama, K. Kohri, and K. Nakayama, *Prog. Theor. Phys.* **126**, 331 (2011) [arXiv:1102.5612]; S. Clesse and B. Garbrecht, *Phys. Rev. D* **86**, 023525 (2012) [arXiv:1204.3540].
- [30] G. Lazarides and Q. Shafi, *Phys. Lett. B* **258**, 305 (1991); K. Kumekawa, T. Moroi and T. Yanagida, *Prog. Theor. Phys.* **92**, 437 (1994) [hep-ph/9405337]; G. Lazarides, R.K. Schaefer and Q. Shafi, *Phys. Rev. D* **56**, 1324 (1997) [hep-ph/9608256]; V.N. Şenoğuz and Q. Shafi, *Phys. Rev. D* **71**, 043514 (2005) [hep-ph/0412102].